Journal of Cerebral Blood Flow & Metabolism (2014), 1–11
© 2014 ISCBFM All rights reserved 0271-678X/14 $32.00
www.jcbfm.com

ORIGINAL ARTICLE

Imaging reveals the focal area of spreading depolarizations and a variety of hemodynamic responses in a rat microembolic stroke model

Zsófia Bere[1,2], Tihomir P Obrenovitch[1], Gábor Kozák[1], Ferenc Bari[1] and Eszter Farkas[1,2]

Spreading depolarizations (SDs) occur in stroke, but the spatial association between SDs and the corresponding hemodynamic changes is incompletely understood. We applied multimodal imaging to visualize the focal area of selected SDs, and hemodynamic responses with SDs propagating over the ischemic cortex. The intracarotid infusion of polyethylene microspheres ($d = 45$ to 53 μm) produced multifocal ischemia in anesthetized rats ($n = 7$). Synchronous image sequences captured through a cranial window above the frontoparietal cortex revealed: Changes in membrane potential (voltage-sensitive (VS) dye method); cerebral blood flow (CBF; laser speckle contrast (LSC) imaging); and hemoglobin (Hb) deoxygenation (red intrinsic optical signal (IOS) at 620 to 640 nm). A total of 31 SD events were identified. The foci of five SDs were seen in the cranial window, originating where CBF was the lowest (56.9 ± 9%), but without evident signs of infarcts. The hyperemic CBF responses to propagating SDs were coupled with three types of Hb saturation kinetics. More accentuated Hb desaturation was related to a larger decrease in CBF shortly after ischemia induction. Microsphere-induced embolization triggers SDs in the rat brain, relevant for small embolic infarcts in patients. The SD occurrence during the early phase of ischemia is not tightly associated with immediate infarct evolution. Various kinetics of Hb saturation may determine the metabolic consequences of individual SDs.

Journal of Cerebral Blood Flow & Metabolism advance online publication, 30 July 2014; doi:10.1038/jcbfm.2014.136

Keywords: cerebral hemodynamics; imaging; intrinsic optical imaging; spreading depression; voltage-sensitive dyes

INTRODUCTION

Spreading depolarization (SD) is a slowly propagating wave of intense depolarization that travels across the cerebral gray matter and is typically coupled with local changes in cerebral blood flow (CBF). The characteristic features of SD routinely recorded in the laboratory or at the bedside of patients are an obvious, transient negative shift of the slow electrical potential and the concomitant silencing of brain electrical activity known as spreading depression.[1–3] At the tissue level, SD is a selfpropagating cellular ionic imbalance, which travels across the gray matter at a rate of 2 to 6 mm/min.[4] When neurovascular coupling is intact, SD is associated with an apparent, functional hyperemic response.[5] Conversely, when neurovascular coupling is compromised (e.g., by ischemia), the SD-related hemodynamic response becomes atypical, and may shift to hypoperfusion.[6,7]

Spreading depolarization appears not to be harmful to the gross integrity of the nervous tissue under physiologic conditions,[8] but increasing amount of clinical and experimental data suggests that ischemia-related SDs are part of the pathophysiology of cerebrovascular diseases and predict worse outcome.[9] For instance, clinical studies proposed a link between SD clusters and delayed ischemic neurologic deficit after subarachnoid hemorrhage,[10] and experimental findings showed a linear correlation between the number or duration of SDs and the infarct volume after middle cerebral artery occlusion (MCAO) in rats.[11,12] Spreading depolarizations may exacerbate ischemic injury *via* related atypical hemodynamic responses, especially when prolonged hypoperfusion propagates with an SD ('spreading ischemia') as a result of inverse neurovascular coupling.[13] Therefore, careful examination of the SD-associated hemodynamic responses is necessary to promote our understanding of the pathophysiology of SD.

The features of ischemia-induced SDs have been widely examined, yet their site of elicitation (focus) was seldom captured, mainly because of the unpredictability of its location, and the lack of suitable technology. To assess the characteristic features of ischemia-induced SDs at high spatio-temporal resolution, we have developed a live, multimodal imaging technique to capture SDs (i.e., negative shift in membrane potential) and related hemodynamic changes in a closed cranial window created above the rat frontoparietal cortex.[14] Our previous imaging studies that used global forebrain ischemia models revealed SDs propagating across the field of view.[14,15] However, two specific concerns urged us to refine our experimental paradigm: (1) SD foci were not detected in the field of view, because all SDs invaded the cranial window from an unidentified origin; (2) ischemia was homogeneous in the cortical area under study, preventing us to examine the propagation of SDs over areas with varying degree of ischemia.

[1]Department of Medical Physics and Informatics, Faculty of Medicine and Faculty of Science and Informatics, University of Szeged, Szeged, Hungary and [2]Department of Physiology, Faculty of Medicine, University of Szeged, Szeged, Hungary. Correspondence: Dr E Farkas, Department of Medical Physics and Informatics, University of Szeged, Korányi fasor 9, Szeged 6720, Hungary.
E-mail: farkas.eszter.1@med.u-szeged.hu
This study was supported by grants from the EGT Norwegian Financial Mechanisms (NFM, NNF 78902), the Hungarian Scientific Research Fund (OTKA 81266), and the Hungarian National Development Agency (TÁMOP-4.2.2.A-11/1/KONV-2012-0060 and TÁMOP-4.2.2A-11/1/KONV-2012-0052).
Received 5 May 2014; revised 11 June 2014; accepted 2 July 2014

For these reasons, the introduction of an appropriate focal ischemia model was required.

The rat MCAO model for stroke is a widely used method to study the pathogenesis of focal brain infarcts.[16] Moreover, SDs are readily generated after MCAO, which renders the model suitable for the investigation of ischemia-induced SD.[17] Yet, the core of the infarct that is produced by this approach falls more lateral than the position of the cranial window created on the parietal bone of the rat, therefore the potential site of SD elicitation escapes direct imaging. As an alternative to MCAO, the microsphere-induced, multifocal stroke model in rats has been utilized to mimic the formation of small, permanent cerebral emboli and multiple infarct areas.[18,19] Such a multifocal stroke model appears to be more suitable to capture SD elicitation sites in the parietal cortex of the rat. The model is relevant for small embolic infarcts in patients, complications with cardiac or pulmonary arteriovenous shunts (e.g., cerebral emboli), and possibly multiinfarct dementia. Whether SDs occur in microsphere-induced, multifocal stroke in the rat brain has not been shown, but recurrent SDs were successfully evoked in the microembolized mouse brain.[20]

Taken together, our major goals were (1) to determine whether SDs are part of the pathophysiology of microsphere-induced, multifocal stroke, (2) to characterize SD elicitation, and evolution with respect to SD focus, (3) to illustrate patterns of SD propagation over cortical areas with various severity of ischemia, and (4) to reveal the complexity of hemodynamic responses associated with ischemia-induced SDs. To achieve these goals, we utilized our multimodal imaging approach to investigate SDs in a multifocal, microsphere-induced stroke model in the rat.

MATERIALS AND METHODS

Surgical Procedure

Animal procedures were approved by the Ethical Committee for Animal Care of the University of Szeged adhering to national regulation (guidelines of the Scientific Committee of Animal Experimentation of the Hungarian Academy of Sciences, updated Law and Regulations on Animal Protection (40/2013. (II. 14.) Korm) of Hungary), following the EU Directive 2010/63/EU. Thirteen male Sprague-Dawley rats (300 to 450 g, 2 to 3 months old, obtained from the Husbandry of the University of Szeged) were anesthetized with 1.5% to 2.0% halothane in N_2O:O_2 (2:1). Breathing was spontaneous throughout surgical preparation and subsequent data acquisition, and body temperature kept between 37.1°C and 37.4°C using a feedback-controlled heating pad. The right femoral artery was cannulated for the monitoring of mean arterial blood pressure and blood gases. A ventral midline incision was made in the neck to expose the right common carotid artery. A polyethylene catheter (1.0 mm OD × 30 cm Intravenous Cannula, Sims Portex, Smith Indrustries, Hythe, Kent, England) was guided into the right common carotid artery and was advanced gently into the internal carotid artery until it reached the base of the skull. Even though cannula insertion into the common carotid artery blocks blood flow through the artery, the circle of Willis affords compensation to some extent in the rat; the conceivable reduction in perfusion pressure alone did not trigger SD (see Data analysis).

The midline wound was closed, animals were placed in a stereotactic frame, and a cranial window (~4 × 4 mm) was prepared on the right parietal bone with a high-precision electrical drill (Technobox 810, Bien-Air Dental SA, Bienne, Switzerland). An acrylic dental cement ring was built around the craniotomy, incorporating a perfusion inlet and outlet. The chamber was filled with artificial cerebrospinal fluid (mmol/L concentrations: 126.6 NaCl, 3 KCl, 1.5 $CaCl_2$, 1.2 $MgCl_2$, 24.5 $NaHCO_3^-$, 6.7 urea, 3.7 glucose, bubbled with 95% O_2 and 5% CO_2 to achieve a constant pH of 7.45) and the dura was dissected carefully. The window was covered with a glass coverslip glued to the dental cement ring. The cranial window was continuously perfused with artificial cerebrospinal fluid at a rate of 25 μL/min until the start of data acquisition.

Multimodal Imaging

A multimodal imaging system, developed previously in our laboratory, was used to collect information on synchronous changes in membrane potential and related hemodynamic variables.[14] Cellular membrane potential was visualized by using a voltage-sensitive (VS) dye (RH-1838, Optical Imaging Ltd., Rehovot, Israel) whose fluorescence intensity increases with decreasing membrane potential. Changes in cortical CBF and blood flow in small pial arterioles were acquired with LSC imaging. Cerebral blood volume (CBV) in the cortex covered by the cranial window was assessed using IOS evoked with 540 to 550 nm green light illumination: decreasing green IOS intensity (i.e., decreasing intensity of reflected light) was expected to correlate with increasing CBV. Hemoglobin deoxygenation was recorded with the help of IOS under 620 to 640 nm red light illumination: decreasing red IOS intensity represented decreasing Hb saturation; in case Hb was totally desaturated, red IOS intensity changes followed that of CBV.[14] The technical parameters of the experimental set-up, conceptual background of the methodology, equipment used, and image capturing settings were reported previously,[14] and applied without alteration.

Local changes in VS dye fluorescence, CBF, and IOS at red and green illumination with time were determined by placing selected areas of interest (AOIs, 6 × 6 pixel size) on the images. The position of AOI was random for general data assessment (see Types of hemodynamic response of propagating spreading depolarizations), and carefully selected when the focus of an SD (see section Analysis of the focal area of spreading depolarizations) or distinct SD evolution (see sections Propagating spreading depolarization gradually extinguishes over its course and Spreading depolarizations avoid cortical regions with low perfusion) was analyzed. For the extraction of the kinetic of changes, the same selected AOI was used with the four image sequences that were acquired simultaneously. The average gray level within an AOI was measured in individual frames constituting each image sequence, and plotted against the corresponding time of data acquisition.

Experimental Protocol

After loading and wash-out the surplus VS dye from the cranial window, continuous, simultaneous recording of optical signals was performed. After 10 minutes of baseline, cerebral embolism was induced[18] by infusing 45 to 53 μm diameter microspheres (UVPMS-BY2 45 to 53 μm, Cospheric, Santa Barbara, CA, USA), suspended in 0.02% Tween-20 solution (2,000 particles/0.6 mL vehicle) *via* the internal carotid artery cannula, at a rate of 300 μL/min. Optical signals were captured at 1 Hz for 60 minutes after ischemia induction. Each experiment was terminated by halothane overdose, and recording was pursued for another 10 minutes after cardiac arrest.

Histology

To confirm the evolution of ischemic lesions in the model used, seven male Sprague-Dawley rats (360 to 430 g) were anesthetized with 1.5% to 2.0% isoflurane in N_2O:O_2 (2:1). Twenty-four hours after ischemia induction as described at section Surgical procedure, the animals were decapitated in deep anesthesia, their brains quickly removed and rinsed in ice-cold 0.1 mol/L phosphate-buffered saline. The forebrains were positioned into a rodent brain matrix and sectioned in the coronal plain with microtome blades. Brain slices (2 mm thick) were incubated in a solution of 2% 2,3,5-triphenyltetrazolium chloride (TTC) in 0.1 mol/L phosphate-buffered saline for 20 minutes at room temperature. The sections were subsequently immersed and stored in 4% paraformaldehyde. The presence of ischemic infarcts was confirmed, and brain regions involved in infarct maturation were identified.

Because TTC staining may not be sensitive enough to detect micro-infarcts,[20] 5-μm-thick paraffin sections of the TTC-stained slices were obtained, stained with hematoxylin/eosin (H&E), and examined with optical microscopy. The sections were digitally recorded with a microscope slide scanner (Zeiss Mirax Midi Slide Scanner, Carl Zeiss MicroImaging GmbH, Jena, Germany).

Data Analysis

Several rats were excluded from data analysis: In four animals, microspheres did not appear in the cranial window, and SDs did not occur during the observation period, either. These four rats were considered as a control for the surgical procedures and potential photodynamic damage that the illumination paradigm might have caused. Additional two animals were excluded because SDs evolved due to surgical preparation (i.e., air emboli reached the brain due to the insertion of the carotid cannula), prior ischemia induction. In these two rats, ischemia was severe and SDs occurred at a very high frequency. Taken together, 7 of 13 rats were used for full data analysis.

© 2014 ISCBFM

Cerebral blood flow variations were expressed as % of changes with respect to baseline (100%), and residual LSC signal after cardiac arrest taken as zero (0%). Relative CBF changes associated with ischemia induction were analyzed over the parenchyma by categorizing the pixels of the analyzed field of view based on the rate of CBF decrease.[21] The percentage of areas where CBF decreased to $<40\%$, 40% to 50%, 50% to 60%, 60% to 70%, 70% to 80%, 80% to 90%, 90% to 100%, or $>100\%$ of the preischemic baseline was determined (Figures $1C_1$ to $1C_2$).

Cerebral blood flow changes associated with SD, and changes in the other optical parameters were acquired at selected AOIs. The shifts of optical signal intensities (i.e., changes in VS dye fluorescence, and green and red IOS) were expressed as changes in gray levels. Data are given as mean ± s.d. A one-way analysis of variance (ANOVA) paradigm of the software IBM SPSS Statistics for Windows, Version 20.0. (IBM Corp., Armonk, NY, USA) was applied for statistical data analysis. Fisher *post hoc* test was applied for group comparisons where more than two data sets were evaluated. A Wilcoxon signed rank test was used for the analysis of nonparametric data.

RESULTS

Characterization of Cerebral Ischemia

Ischemia achieved by the infusion of microspheres was expected to become multifocal, as a result of the obstruction of cerebral arterioles at multiple sites.[18] Physiologic variables acquired during early ischemia fell within the normal range except for the lower partial pressure of CO_2 (mean arterial blood pressure: 100 ± 11 mm Hg; blood pH: 7.50 ± 0.04; pO_2: 151 ± 15 mm Hg; pCO_2: 16.9 ± 7.8 mm Hg). During the infusion of microsphere suspension, the inflow and capture of microspheres in pial arterioles could be followed in the area revealed by the cranial window (Figures $1B_1$ and B_2). Blood flow measurements in representative pial arteriolar segments showed that blood flow clearly decreased distal to microsphere capture (Figures $1B_1$ to B_4).

Ischemia developing in the visualized part of the cerebral cortex was estimated with the help of CBF measurements. The magnitude of CBF reduction immediately after ischemia induction showed considerable heterogeneity within and between experiments (Figures $1C_1$ and C_2): as an average, CBF decreased below 50% in ~8% of the cortical area revealed by the cranial window, varied between 50% and 90% in ~61% of the cortical area, and remained above 90% in around 31% of the visible cortex (Figure $1C_3$).

Examination of TTC-stained forebrain slices confirmed infarct evolution 24 hours after ischemia induction in five of seven animals used for this purpose: three animals developed extensive infarcts in ipsilateral cortex, hippocampus, and subcortical gray matter (Figure $1A_2$), two additional rats had smaller, distinct, focal lesions in the ipsilateral frontoparietal cortex (Figure $1A_1$), which was also confirmed in H&E sections (Figures $1A_3$ and $1A_4$). Two of seven animals did not show any signs of macroscopic infarctions in TTC slices, and no microinfarctions were detected in the H&E-stained sections, either. These two rats most probably represent cases, in which microspheres failed to reach the brain (see section Data analysis).

Characterization of Spreading Depolarizations and Associated Hemodynamic Responses

Spreading depolarizations were identified as a marked, rapid increase in VS dye fluorescence intensity propagating across the field of view at a rate typical of SD, as described previously.[22] In total, 31 SDs were recorded in 7 experiments. All the observed SDs appeared to be related to ischemia, since they occurred after the induction of multifocal ischemia. The number of SDs during the period of observation (i.e., 1 hour) ranged from 2 to 12 events per experiment. The foci of five SDs were seen within the cortical area revealed by the cranial window; all the other SDs invaded the area from a distant origin.

Analysis of the focal area of spreading depolarizations. The localization of the elicitation sites (foci) of SDs within the cranial window offered the possibility to examine SD features at the proper focus, and at increasing distances (200 to 1,500 μm) from the SD focus of each event. The five SDs originating in the field of view were captured in four different rats: in one rat, two SD foci were seen (first and fourth SDs, the focal sites were spatially near each other but not identical). Spreading depolarizations originating in the cranial window emerged either as the first event in a sequence of SDs (e.g., in tissue not involved in the evolution of prior SDs; $n=2$) or at sites that had been involved in the spreading of prior SDs ($n=3$). Their average latency with respect to ischemia induction was 20.4 ± 17.6 minutes. The waves propagated in a radial manner. Three of the five SDs emerged as short, transient depolarizations, one as an intermediate, transient depolarization (Figures 2 and 3A; duration: 3.26 minutes), and one as persistent depolarization (i.e., no recovery of membrane potential till the next event), as indicated by the VS dye signal extracted at the proper focus. The intermediate and terminal SDs converted into short, transient depolarization as they propagated away from the focus (conversion observed at a distance of 1 to 1.5 mm with respect to the focus; Figure 3A). The rate of propagation tended to decelerate as depolarizations were spreading (from 6.5 ± 4 mm/min near the focus to 3.9 ± 1.6 mm/min ~1 mm away from the focus; Figure 3B). The site of terminal SD focus did not substantiate the propagation of subsequent SDs, but the other foci displaying transient SD features were involved in the propagation of subsequent SD waves.

Spreading depolarizations were typically elicited at a site where CBF before SD elicitation was the lowest in the field of view (56.9 ± 9%). Local CBF measured shortly before SD evolution increased with the distance from the site of SD elicitation, and was as high as 86.9 ± 18.7% 1 mm away from the SD focus, with respect to 56.9 ± 9% at the proper focus (Figure 3C). The typical SD-associated hyperemia was totally absent ($n=3$; Figure 3A) or minor ($n=2$) at the site of elicitation, irrespective of the duration of the depolarization. The magnitude of SD-related hyperemia increased with the distance from the SD focus (Figure 3D). Cerebral blood flow returned to the pre-SD level after the passage of the hyperemic response.

Features of propagating spreading depolarizations. The VS dye signature of SDs illustrated that each propagating SD that arrived at the cranial window from a distant origin was a transient, negative shift in membrane potential. The rate of propagation decreased between 1.8 and 6.2 mm/min (3.02 ± 1.08 mm/min). The dominant site of SD entry into the cranial window was frontal/frontolateral ($n=19$). A few SDs invaded the area from the lateral edge of the cranial window ($n=5$), and only two events arrived from a caudal direction. The dominant direction of propagation was, thus, frontal-to-caudal. The site of SD entry to the cranial window was not conserved within individual experiments; in addition, propagating SDs were interspersed with SDs emerging in the cranial window, implying multifocal SD origin in the ischemia model used.

Since the course of evolution for individual SDs was found to be highly variable, representative examples are presented below to illustrate the distinct phenomena observed.

Propagating spreading depolarization gradually extinguishes over its course. Several SDs in four experiments diminished while propagating across the visible part of the cortex. Figure 4 shows the evolution of one of these particular SDs as it was traveling over a distance of 2 mm. Cerebral blood flow right before SD elicitation was 60% of baseline, which was relatively uniform over the field of view. The peak of SD-related hyperemia was 130% of baseline at the site nearest SD entry to the cranial window, which became gradually less pronounced as the wave advanced over the cortex. At the most distant sampling site with respect to SD entry to the cranial window, the VS dye signature of SD did not indicate any

© 2014 ISCBFM

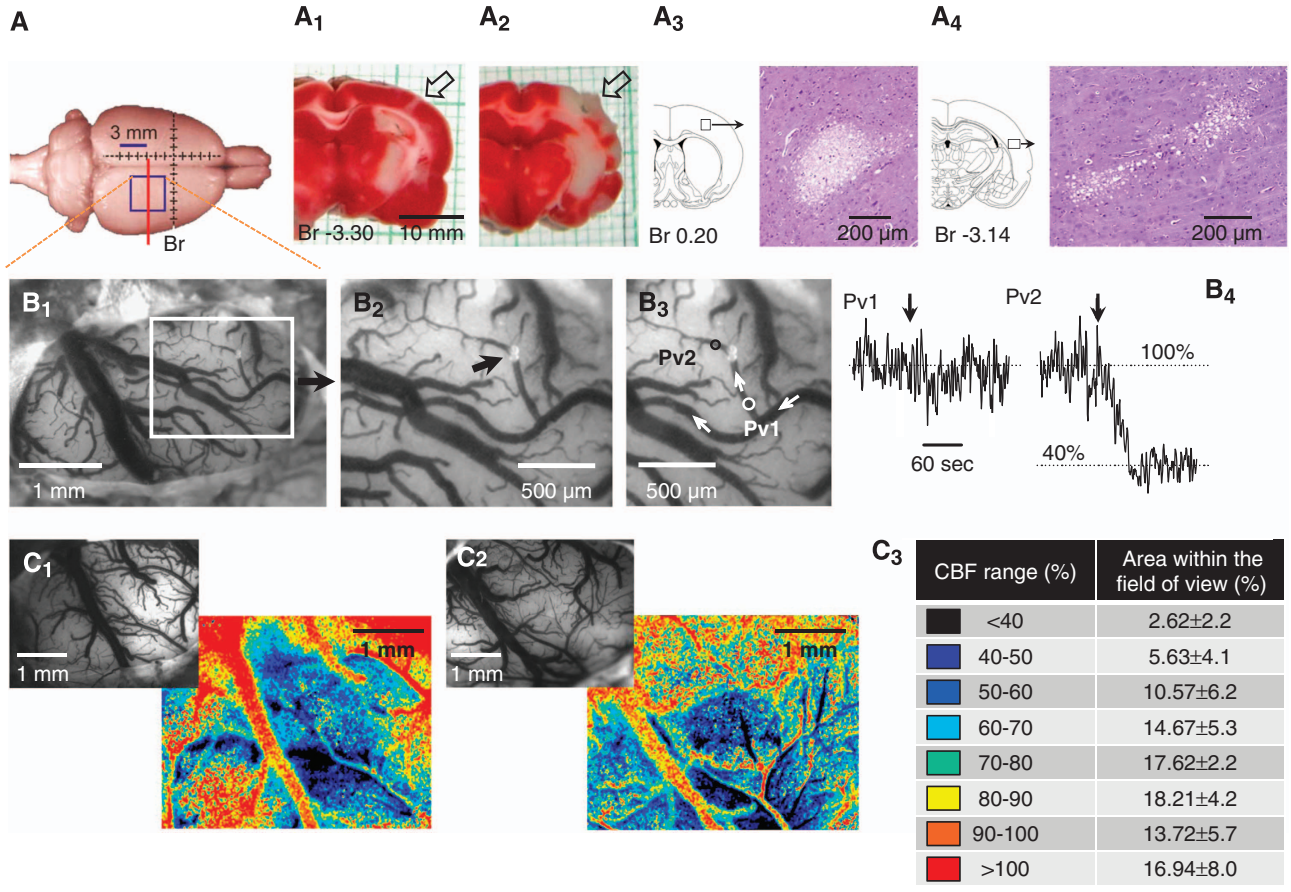

CBF range (%)	Area within the field of view (%)
<40	2.62±2.2
40-50	5.63±4.1
50-60	10.57±6.2
60-70	14.67±5.3
70-80	17.62±2.2
80-90	18.21±4.2
90-100	13.72±5.7
>100	16.94±8.0

Figure 1. Representative images and graphs illustrate the reduction in blood flow in the pial arterioles and brain parenchyma within the whole field of view after microsphere capture in pial arterioles. (**A**) The blue rectangle on the right parietal cortex indicates the position of the cranial window; the red vertical line crossing the rectangle represents the plane of 2,3,5-triphenyltetrazolium chloride (TTC)-stained coronal sections shown in panels (**A_1** and **A_2**). Vertical bar with scaling represents bregma (Br). Panels (**A_1** and **A_2**) show TTC-stained coronal brain slices representative of focal infarction in the cortex (**A_1**), and extensive infarction in the cortex (**A_2**), indicated by arrows. Panels (**A_3** and **A_4**) show cortical microinfarcts as revealed by hematoxylin/eosin staining. (**B_1**) Vascular architecture of the brain surface in the cranial window, as revealed by green light (540 to 550 nm) reflection. The image was taken after microspheres had appeared in pial arterioles. (**B_2**) Two adjacent microspheres ($d = 45$ to 56 μm) captured in a pial arteriole are pointed to by an arrow. (**B_3**) In a representative image reproduced from panel (**B_2**), small circles indicate sampling sites (areas of interest, AOIs) positioned on arteriolar segments: Pv1 proximal to microsphere capture (arteriolar diameter at baseline: 50 μm), and Pv2 distal to microsphere capture (arteriolar diameter at baseline: 33 μm). These AOIs were used to extract the kinetics of changes in arteriolar blood flow, which was assessed in separate videos created by laser speckle contrast (LSC) analysis. White arrows show the direction of blood flow. (**B_4**) Traces of pial arteriolar flow (obtained by LSC analysis), corresponding to the sites of sampling given in panel (**B_3**). Vertical arrows indicate the time of microsphere capture in the arteriole. Note the reduction in blood flow (from 100% to 40%) distal to the site of microsphere capture. Note that the magnitude of arteriolar flow reduction could be underestimated, as cerebral blood flow (CBF) signal arising from the underlying parenchyma might have contributed to the arteriolar flow signal, especially when arteriolar flow was diminishing. Panels **C** (**C_1** and **C_2**) show two examples for whole field analysis of CBF maps to reveal the heterogeneity of ischemia evolution within the field of view: small black-and-white images show the vascular architecture of the brain surface in the cranial window at baseline for anatomic orientation (540 to 550 nm illumination); color-processed images provide the false-colored flow map (based on LSC analysis) of the same area after ischemia induction. Relative CBF was expressed in the percentage of baseline; color coding of CBF ranges is depicted in the table in (**C_3**). Note uneven perfusion conditions in these images. The table in (**C_3**) summarizes the average size of surface area of brain parenchyma (i.e., visible vessels excluded) with different ranges of relative CBF (mean ± s.d., $n = 7$).

shift in membrane potential, and the associated CBF signal showed no variation, either. The changes in green and red IOS evolved parallel with the shifts in VS dye fluorescence and CBF: the SD-related decrease in green and red IOS (increase in CBV and Hb desaturation, respectively) became gradually smaller over the course of SD propagation.

Spreading depolarizations avoid cortical regions with low perfusion. In two experiments (in which sequences of three or four SD events were recorded), it was clearly seen in videos that several SDs curved around patches of the cortex as they propagated. A representative SD is depicted in Figure 5. The kinetics of optical signals (for VS dye, green and red IOS) and CBF were extracted at selected sites conserved for all signals (Figure 5A). The traces at several of these sites confirmed the occurrence of SD (Figure 5D). The lack of signature of the propagating SD on all signals corresponded with the region avoided by the SD as seen in the videos (Figures 5C and 5D).

In these particular experiments, CBF in the cortex estimated right before SD elicitation showed areas of higher and lower values ranging between 40% and 100% of baseline. In the representative example, the incoming SD curved around regions showing the lowest CBF (~40% of baseline, deep blue in Figure 5C). Terminal depolarization was not detected in these regions during image acquisition, before the occurrence of recurrent SDs.

© 2014 ISCBFM

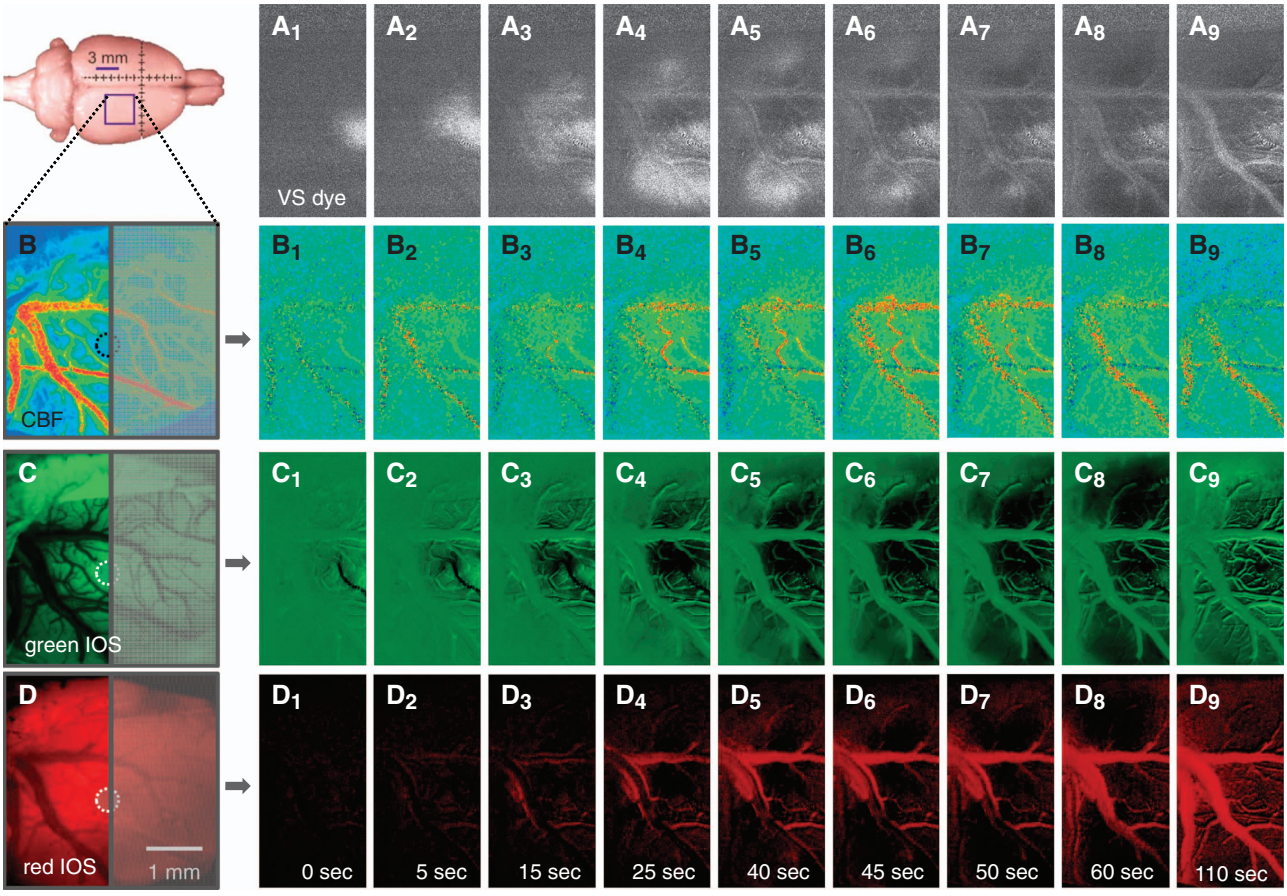

Figure 2. Representative image sequences in the four variables under study, recorded during the initiation and propagation of a spreading depolarization (SD) event originating in the cranial window. The square placed on the rat brain in the upper left hand corner depicts the position and size of the cranial window. (**A_1** to **A_9**) Voltage-sensitive (VS) dye fluorescence intensity; (**B_1** to **B_9**) Laser speckle contrast (LSC) imaging of cerebral blood flow (CBF); (**C_1** to **C_9**), Change in intrinsic optical signal (IOS) acquired under green illumination (540 to 550 nm) expected to reflect, primarily, changes in cerebral blood volume (CBV); and (**D_1** to **D_9**) Change in IOS under red illumination (620 to 640 nm), which appears to represent hemoglobin oxygenation level. Pictures (**B** to **D**) show the cortical region under study at the various illuminations taken at baseline. These images are averages of 10 consecutive captured images. The right side of the images is partially obscured to highlight the left side, which is displayed in pictures 1 to 9. Dotted circles in (**B** to **D**) represent the focus of SD. Pictures 1 to 9 of the VS dye, CBF, green and red sequences were modified by background subtraction (background taken as the first image of the sequence) followed by contrast enhancement. The image sequences were smoothed throughout the recording period by running average on five consecutive frames. Additional pseudo-color processing was implemented for CBF, green and red IOS. The kinetics of changes in VS dye fluorescence intensity and CBF are depicted in Figure 3 for this particular SD.

Types of hemodynamic response of propagating spreading depolarizations. Two basic types of hemodynamic responses coupled to SDs were defined based on the kinetics of CBF. Transient functional hyperemia developed with most SDs ($n = 30$, Figures 6A to 6C). The mean absolute peak value of the hyperemic response was 129.8 ± 18.6% (with respect to 100% baseline before microsphere infusion), which corresponded with a CBF increase of 54.5 ± 21% relative to CBF preceding SD elicitation (75.3 ± 12.5%). Hypoperfusion was associated with only one SD, which followed ischemia onset with a short delay (Figure 6D). Reduced CBF here did not recover until the elicitation of the subsequent SD (~8 minutes later). The lack of a clear SD-associated hemodynamic response was noted only for the focus of SDs (Figure 6E).

Spreading depolarization-related changes in green IOS representing CBV were synchronous with the variations in CBF: green IOS decreased with hyperemia (increased CBV)—the lowest value being in temporal match with the CBF peak (Figures 6A to 6C), and increased with hypoperfusion (reduced CBV, Figure 6D).

Changes in red IOS intensity representing Hb (de)saturation proved to be more diverse. The signal of 25 SDs was examined in detail. Spreading depolarization-related red IOS variation appeared to be biphasic: an early increase (Hb saturation) in signal intensity coincided with the initial phase of CBF elevation, which was followed by a sharp decrease in red IOS below baseline (Hb desaturation), the start of which preceded the peak of hyperemia. The minimum value of red IOS intensity coincided with the minimum value of green IOS intensity and the peak of hyperemia. On the basis of the dominance of either of the two phases, four types of SD-related red IOS signatures were defined. Hyperemic CBF response was associated with one of the following red IOS signatures: (1) dominant initial phase (i.e., accentuated transient increase in signal intensity, Type 1; $n = 5$, Figure 6A), (2) approximately equal magnitude of the two phases (Type 2; $n = 7$, Figure 6B), and (3) dominant later phase (i.e., major transient reduction in signal intensity, Type 3; $n = 12$, Figure 6C). With SD-related hypoperfusion, red IOS intensity showed a monophasic, marked reduction before the decrease in CBF (Type 4; $n = 1$, Figure 6D).

The Type of red IOS signature that was associated with hyperemic CBF response appeared to be unrelated to the

© 2014 ISCBFM

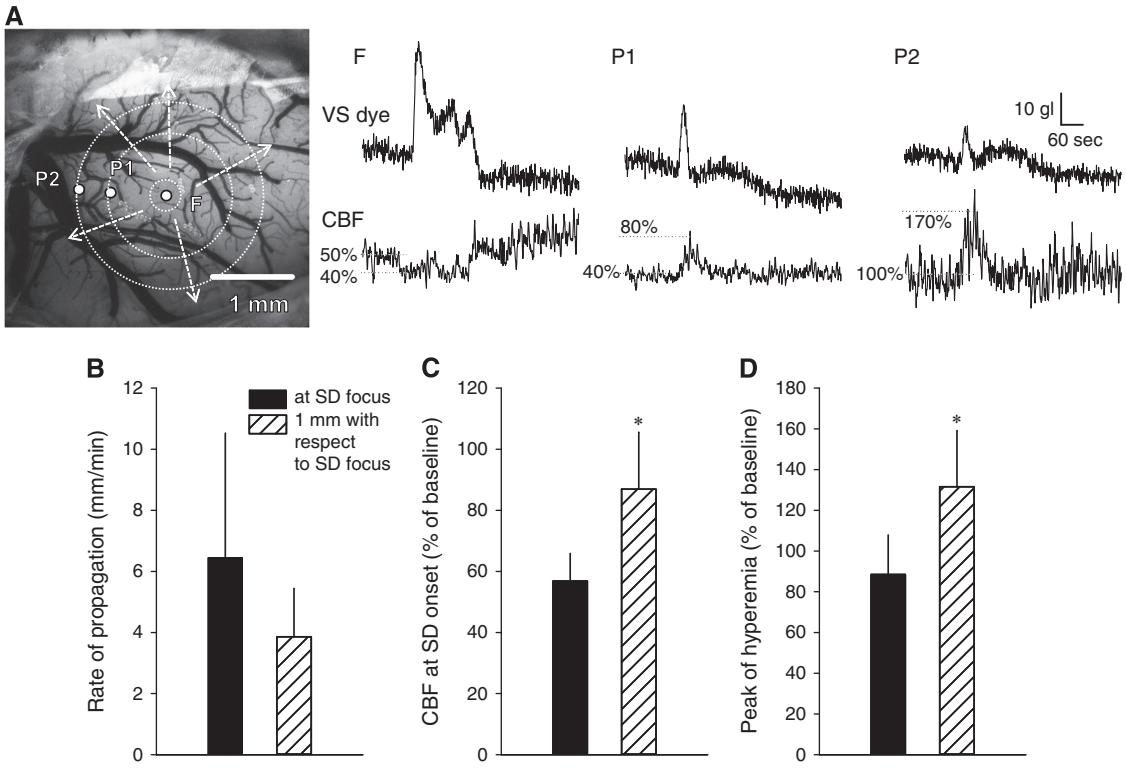

Figure 3. Kinetics of the voltage-sensitive (VS) dye signature and changes in local cerebral blood flow (CBF) associated with spreading depolarization (SD) near its focal area. (**A**) The evolution of a representative spreading depolarization as shown by VS dye and CBF traces taken at the focus of SD (F), and at two selected points (P1 and P2) in the cortex, at increasing distances with respect to SD focus. The position of sampling sites is illustrated in an image (upper left), taken at green light illumination (540 to 550 nm). Circles (white dotted lines) and arrows (white broken lines) in the image show the radial propagation of SD. (**B**) Rate of propagation of SD at the site of SD elicitation (focus) and 1 mm with respect to the focus. (**C**) CBF values taken shortly before SD evolution at SD focus, and 1 mm with respect to SD focus. (**D**) Peak of SD-associated hyperemia at SD focus, and 1 mm with respect to SD focus. Data are given as mean ± s.d. Analysis of variance (ANOVA) was used for statistical analysis (*$P<0.05$ given as level of confidence).

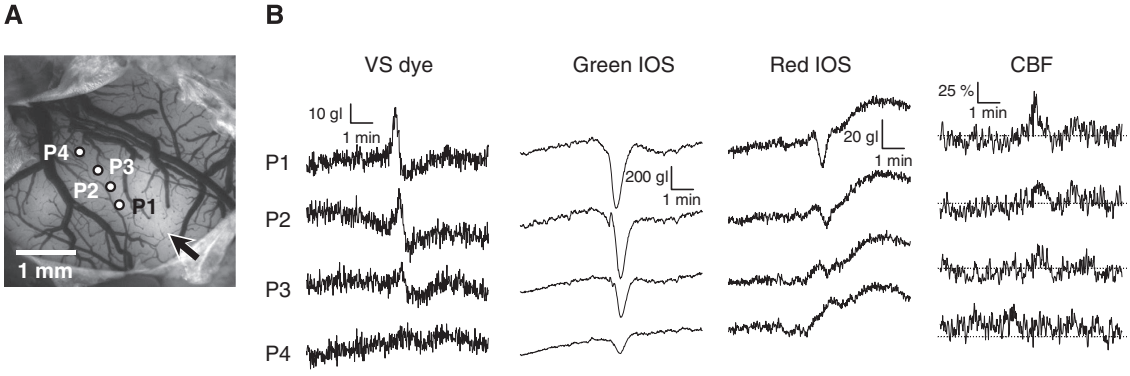

Figure 4. Spreading depolarization (SD) gets extinguished as it propagates across the cortical surface revealed by the cranial window. (**A**) SD (the second event in the given experiment) invaded the cranial window from the frontolateral corner (black arrow) and traveled to the caudomedial corner. Areas of interest (white circles, P1 to P4) were positioned along a line (~400 μm apart), perpendicular to the wave front of SD, parallel with the direction of SD propagation. The position of sampling sites is illustrated in an image taken at green light (540 to 550 nm) illumination. (**B**) Representative traces extracted at the given sites of sampling (P1 to P4 left to the traces) show the kinetics of changes in voltage-sensitive (VS) dye fluorescence, green intrinsic optical signal (IOS), red IOS, and cerebral blood flow (CBF) related to the SD, as it propagated across the field of view. Horizontal dotted line in each CBF trace indicates 60% of baseline CBF. Changes in optical signal intensities for VS dye, green and red IOS are given in gray level (gl).

magnitude of transient hyperemia (ANOVA: $F=0.162$, $P\leqslant0.852$), or CBF values shortly before SD evolution (ANOVA: $F=1.366$, $P\leqslant0.277$), but depended on the magnitude of the initial decrease in CBF at ischemia induction (ANOVA: $F=5.978$, **$P\leqslant0.009$, Figure 6F): a larger decrease in CBF coincided with a more dominant second phase of the signature (transient decrease in red IOS intensity with SD, Hb desaturation). The Type of red IOS signature displayed a less pronounced second phase (Hb desaturation) the

© 2014 ISCBFM

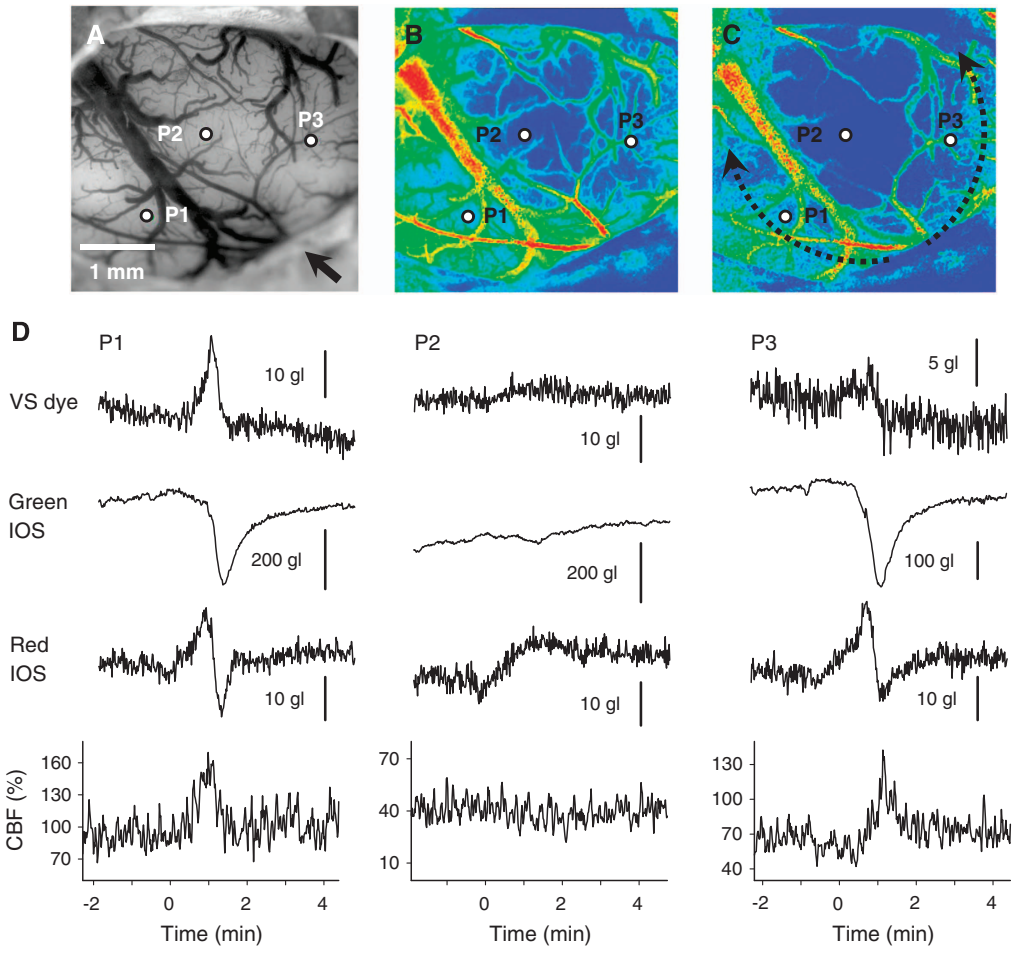

Figure 5. Spreading depolarization (SD) avoids a cortical region undergoing deeper ischemia. The third SD in this particular experiment invaded the cranial window from the frontolateral corner (black arrow) and traveled to the caudomedial corner (**A**). Areas of interest (AOIs) (white circles, P1 to P3) were positioned (~1.36 mm apart) parallel with the wave front of SD. (**B** and **C**) Color-coded cerebral blood flow (CBF) maps derived by pseudo-color application to laser speckle contrast images at baseline (**B**) and right before the occurrence of SD (**C**). Colors range from red to blue, red standing for the highest and blue for the lowest CBF within the images. AOIs (P1 to P3) are drawn to appreciate their position with respect to the relative level of CBF. Black dashed arrows indicate the approximate course of SD around the area coded by deep blue (lowest CBF). (**D**) Representative traces extracted at the given sites of sampling (P1 to P3 indicated at the top) show the kinetics of changes in voltage-sensitive (VS) dye fluorescence, green intrinsic optical signal (IOS), red IOS, and CBF related to the SD, as it propagated across the field of view. Note that no clear sign of SD appears on the optical signals obtained at P2, which is positioned in the cortical area colored deep blue (lowest CBF) in (**C**). Changes in optical signal intensities for VS dye, green and red IOS are given in gray level (gl).

later it appeared in an SD sequence; in other words, the Type of red IOS signature changed in the course of the SD sequence in such a way that the red signal with later SDs contained smaller Hb desaturation element as compared with preceding SDs (Figure 6G).

DISCUSSION

Because there is no evidence that SD spontaneously occurs in the brain under physiologic conditions, SD is regarded to be a pathophysiologic phenomenon. Ischemia is a condition known to favor the elicitation of SD—in turn, SD evolution appears to be harmful to the functional and morphologic integrity of the ischemic nervous tissue.[9,11,12] Much and successful effort has been done recently to dissect the role of SD in brain injury in patients;[2,3] but appropriate animal models are still needed to provide a more comprehensive picture of how SD evolves in the ischemic cortex. The early phase of ischemia may be of special interest, because the early SD events in human ischemia typically escape detection due to the lag between injury onset and the start of data acquisition. Here, we detail our observations concerning SD evolution shortly after the induction of multifocal ischemia in the rat.

Features of the Microembolic Stroke Model

Microsphere-induced embolization is a well-accepted stroke model in rats.[18,19] The degree of perfusion deficit determined shortly after microsphere infusion here was similar to that previously assessed by magnetic resonance imaging in this model.[19] Cerebral blood flow in our study could be assessed in the cortex revealed by the cranial window, but perfusion deficit deeper than that could have evolved in subcortical regions, as shown earlier with magnetic resonance imaging.[19] Long-term follow-up showed that CBF reduction persisted for weeks after microembolization, which was accompanied by the gradual evolution of brain infarcts.[18,19] We also confirmed the presence of infarcted areas in the cortex (the target of our imaging approach) with TTC staining 24 hours after embolization. The present study focused on the first hour after

© 2014 ISCBFM

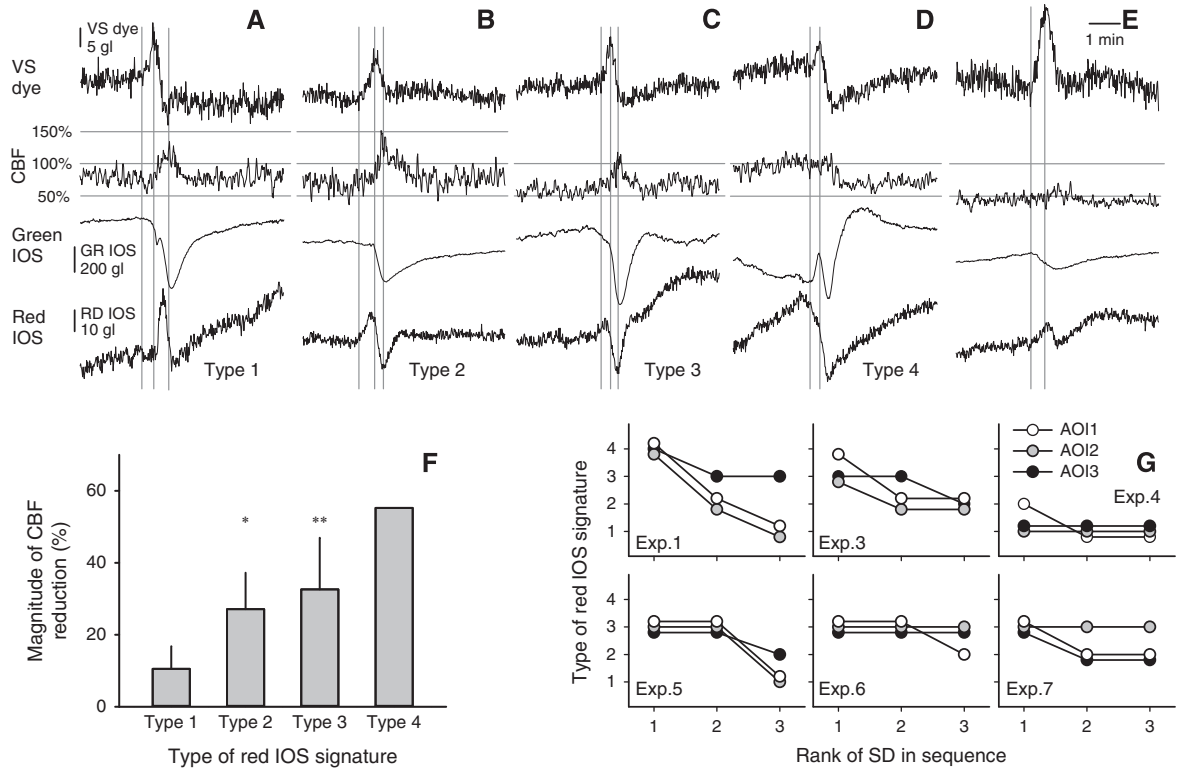

Figure 6. Representative original traces (**A** to **E**) show various types of hemodynamic responses associated with spreading depolarization (SD). Traces show the kinetics of changes in voltage-sensitive (VS) dye fluorescence, cerebral blood flow (CBF), green (GR) intrinsic optical signal (IOS), and red (RD) IOS, related to SD. Vertical gray guidelines help to appreciate the temporal relationship between the kinetics of corresponding optical signals. The guidelines are aligned to the start and peak of the SD related increase in VS dye fluorescence (**A** to **E**), and the peak of associated hyperemia where applicable (**A** to **C**). Changes in optical signal intensities for VS dye, green and red IOS are given in gray level (gl). Red IOS signatures with different kinetics are labeled as Type 1 to 4 (**A** to **D**). The type of red IOS was related to the magnitude of CBF reduction shortly after ischemia induction (**F**). Data are expressed as mean ± s.d. Analysis of variance (ANOVA) followed by Fisher's *post hoc* test revealed significant differences in the initial decrease in CBF associated with different types of red IOS signature (**$P<0.01$ and *$P<0.05$ given as levels of confidence). Statistical analysis was performed for Type 1 to 3, because Type 4 contained one case only. Finally, the type of SD-related red IOS signature was determined for the first three recurrent SDs in individual experiments to show how the type of red IOS signature changes with the rank of SD in SD sequences (**G**). Separate plots depict data obtained at three areas of interest (AOIs) (AOI1, AOI2, and AOI3) in individual experiments (Exp. 1 to 6). One of the seven experiments was excluded from this analysis, because only two SDs occurred, both with Type 1 red IOS signatures. Statistical analysis with the non-parametric Wilcoxon signed rank test (one-tailed) revealed a significant change in the Type of red IOS for the third SD as compared with the first SD (*$P<0.029$).

embolization, during which the achieved perfusion deficit may cause initial microinfarctions,[18] rather than obvious, extensive infarcted regions.[20]

Typical Features of Spreading Depolarizations and Associated Hemodynamic Responses

The focal area of spreading depolarizations. The present study shows the subtleties of the evolution of spontaneously generating SDs during ischemia, in close proximity to their focus. Even though the focus of ischemia-induced SDs was previously identified based on IOS at 550 nm illumination,[23] and LSC imaging,[24] the changes in membrane potential were not determined. Here, we show that the duration of SD (time between depolarization and repolarization) tends to be prolonged at the proper focus compared with sampling sites more distant to the focus, and the rate of SD decelerates with the increasing distance from the focus. The duration of SD is indicative of the energy crisis within the tissue,[25] and the rate of SD propagation is predicted to increase when (1) extracellular K^+ removal is hampered, (2) the extracellular space is smaller (cell swelling), and (3) extracellular K^+ and/or glutamate concentrations are increased.[26] In line with the predictions, hypoxic SDs tended to propagate ~1 mm/min more rapidly than normoxic SDs as observed in brain slices.[27] These data in combination with our findings suggest that the tissue at the SD focus may be at the highest risk for permanent injury.

The present results also revealed that CBF before SD elicitation was the lowest, and the peak of SD-associated hyperemia was smallest at the focus of SDs, as compared with other sites more distant to the focus. These observations imply that in tissue with uniform structure (i.e., rodent cortex), SD is elicited at a site where the reduction in CBF reaches a critical threshold, and subsequently, neurovascular coupling is the least efficient to support functional hyperemia.

The imaging studies that relied on IOS and LSC maps identified the foci of SD-associated optical signal variations at the edge of an evolving ischemic core region.[23,24] In contrast, SD foci revealed in the present study were not associated with the immediate evolution of an evident ischemic core. It is possible that microinfarcts too small for detection with imaging were associated with SD events.[20] However, supportive evidence suggests that the focus of ischemia-induced SD does not necessarily fall near the ischemic core or the thin penumbra embracing it,[28] and milder ischemic insults are able to trigger SD.[29] Finally, tissue at SD foci displaying a transient shift in membrane potential was involved in the propagation of subsequent SDs in our experiments, which

© 2014 ISCBFM

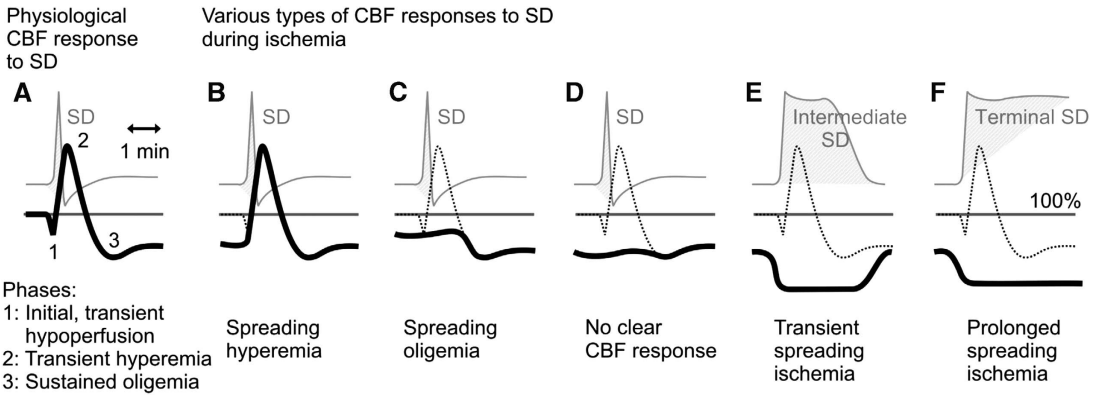

Figure 7. Overview of various conceptual cerebral blood flow (CBF) responses to spreading depolarization (SD) in intact cerebral cortex (**A**), and during ischemia (**B** to **F**). Solid, black lines depict theoretical CBF responses based on our present and previous observations. Dotted lines in (**B** to **F**) indicate the physiologic CBF response to SD, for comparison with those under ischemia. Gray lines and shaded areas stand for ideal SD: short transient in (**A** to **D**), intermediate in (**E**), and terminal in (**F**). Baseline CBF (100%) is given as a horizontal line.

indicates functional recovery from the primary ionic imbalance. This suggests that non-terminal SD in ischemic tissue probably does not cause immediate injury; nonetheless, the reestablished membrane potential may not guarantee ultimate neuronal survival.

Features of Spreading depolarizations over their course of propagation

Propagating Spreading depolarization gradually extinguishes. We showed here that some propagating SDs gradually diminish over their course of traveling over a uniformly perfused cortex. Such diminishing waves were previously seen in the chicken retina *ex vivo*—obviously without the hemodynamic components.[30] Furthermore, the hyperemic response to SD was seen to die away in stroke patients.[31] Still, the exact details as to why some SD waves become gradually smaller and then cease to propagate are not clear. One might speculate that part of the brain tissue is in refractory phase after an SD wave, and may not be able to sustain a subsequent SD. The diminishing waves observed here followed previous, short transient SDs with a delay as long as 8 to 10 minutes, which time span is apparently long enough for the restoration of resting membrane potential, but might prove too short for the complete recovery of the ionic milieu and/or the metabolic status, especially in the ischemic cortex. Alternately, a diminishing SD may propagate against an extracellular ionic gradient that does not support depolarization to evolve (possibly decreasing K^+ levels as a result of enhanced reabsorption, or increasingly higher Mg^{2+} concentrations), and brings the SD to a gradual halt. Finally, hampered water movement through glial aquaporin channels was proposed to counteract the propagation of SD,[32] which may be another potential mechanism to bring SD to cessation.

Spreading depolarizations avoid cortical regions with low perfusion. A few SDs in our experiments avoided a distinct region of the visible cortex. In contrast with the diminishing waves presented above, these SDs were not extinguished gradually, but sharply curved around an area showing the lowest CBF in the field of view, and thus propagated with an irregular wave front. Similar to these observations, magnetic resonance imaging failed to detect the propagation of SD-related signals toward cortical regions with severe tissue perfusion deficit immediately after MCAO in the rat,[28] and LSC imaging identified circumferential propagation of SD-related flow responses around areas defined as primary ischemic core regions in rats and cats.[24] According to our best knowledge, an SD does not invade a bulk of tissue if (1) the area has depolarized terminally (therefore subsequent depolarization cannot occur) or (2) the area is suffering of ongoing epileptic activity.[33] Primary infarct evolution in the area avoided by SDs was not seen in our experiments (i.e., signature of potential terminal depolarization was not acquired), therefore infarct maturation is not held responsible for the obstruction of SD propagation. Focal seizures are known as potential consequences of ischemic brain injury,[34] and microembolization in the rat has been shown to induce seizures,[35] but the methods applied here did not allow observations to justify or exclude seizure activity. All things considered, presently we can only claim that the area not being able to substantiate SD propagation was of the lowest perfusion within the field of view, but was presumably not infarcted.

Types of hemodynamic response to spreading depolarizations on their course of propagation. The characteristic features of the SD-associated hemodynamic response have been the target of intensive research, because atypical CBF variation during ischemia is believed to aggravate metabolic supply-demand mismatch and appears to be potentially harmful to the tissue.[9]

Two distinct patterns of CBF responses associated with propagating, transient SDs were identified: spreading, transient hyperemia (Figures 6A to 6C), and spreading, prolonged hypoperfusion (Figure 6D). In the rat, the physiologic pattern of CBF changes coupled to SD includes an initial, brief decrease in CBF; a marked, transient hyperemia; and a sustained hypoperfusion also known as spreading oligemia[36] (Figure 7A). The above three elements of the SD-related CBF response are assumed to be the result of a sequence and combination of separate vasoregulatory mechanisms.[36]

Superimposed on ischemia, the SD-related CBF response becomes atypical. The type of CBF response most frequently seen here displayed the hyperemic element only. The initial, brief decrease in CBF is known to disappear with recurrent SDs in close succession,[36] which may be applicable for our model (i.e., repeated SDs propagated over the cortex). Further, we speculate that both the initial, brief decrease in CBF and the final prolonged oligemic component remained obscure during ischemia, because CBF shortly before SD occurrence was already low due to the created perfusion deficit (Figure 7B).

One transient SD event that occurred shortly after ischemia induction was followed by prolonged hypoperfusion in this study (Figure 6D). Previously, spreading ischemia was suggested to develop by the domination of the initial hypoperfusion over the subsequent, diminishing hyperemic element of an SD-related CBF response,[7,36] which implies that the onset of spreading ischemia should fall on the depolarization phase of SD (Figures 7E and 7F). Yet, the onset of hypoperfusion here coincided with the hyperpolarization phase of SD (Figure 6D). This delayed onset

© 2014 ISCBFM

may suggest that the decreasing CBF was essentially the lower segment of the downward slope of a fictional hyperemic peak (thus, without the actual evolution of a clear hyperemia due to hampered vasodilation), which turned into spreading oligemia (the third element of a CBF response) (Figure 7C). In addition, it is a necessary electrophysiologic criterion for spreading ischemia that the SD event, to which it is related, must be prolonged.[9] On the basis of our current observation and the previously set criterion, it is important to point out that an SD-associated decrease in CBF is not automatically a sign of spreading ischemia.

Finally, no discernable variation in CBF was seen at the focus of a few SDs (Figure 6E). We propose that the SD-related CBF response may escape detection when CBF shortly before SD occurrence is already low as part of the ischemic condition, and vasodilatory mechanisms responsible for the evolution of hyperemia are suppressed or disabled (Figure 7D).

The diverse kinetics of changes in red IOS intensity (representative of Hb saturation) with transient hyperemia (Figures 6A to 6C) denotes various metabolic consequences of SDs in the ischemic cortex. Because the Type 1 to 3 red IOS intensity changes were all coupled to transient hyperemia, and the types of red IOS signature were unrelated to the magnitude of hyperemia, the analysis of the kinetics of hyperemic CBF responses alone appears not to be sufficient to draw conclusions about the metabolic consequences of SD. The type of red IOS signature was related to the magnitude of CBF reduction caused by ischemia induction (Figure 6F). This and the above observations suggest that the metabolic consequences of SD with a hyperemic response depend more strongly on the severity of ischemia, than the characteristics of the SD-coupled CBF variation.

In the nonischemic cortex, red IOS changes coupled to KCl-induced SD resemble the Type 2 variation shown here[37] (Figure 6B), which corresponded to a 15% to 20% SD-associated decrease in the concentration of deoxygenated Hb (HbR).[37,38] Type 1 red IOS signature refers to an even more pronounced decrease in HbR concentration (i.e., dominating increase in red IOS intensity) synchronous with increasing local CBV (i.e., reduction in green IOS intensity), which indirectly refers to Hb saturation. The Hb saturation with the SD-related hyperemia might promote the oxidative substrate-dependent recovery from SD; consequently, such hyperemic CBF responses may be protective. Since Type 1 and 2 red IOS variations were coupled to half of the observed SDs, a fraction of ischemia-induced SDs is suggested to have metabolic consequences that may be beneficial to the ischemic tissue.

However, Type 3 and 4 red IOS signatures represent a more accentuated increase in HbR concentration (dominant decrease in red IOS intensity), similar to the SD-coupled HbR dynamics previously acquired by near infrared spectroscopy in the ischemic rat cortex.[39] This pattern of IOS changes may correspond with the reduction cycle of NADH with SD reported during oxygen deficiency,[25] which would indicate metabolic crisis. Taken together, SDs with Type 3 and 4 red IOS signatures are suspected to be malignant.

Finally, the Type of SD-related red IOS signature indicated a less pronounced decrease in HbR concentration with the increasing rank of SD in an SD sequence (Figure 6G), which is taken as a sign of progressive metabolic recovery during the SD sequence. This challenges the view of an inevitable cumulative metabolic failure with recurrent SDs in the ischemic cortex.

CONCLUSIONS

We have shown that microsphere-induced embolization gives rise to spontaneous, recurrent SDs in the rat cerebral cortex. This indicates that SDs could evolve in small embolic infarcts in patients, complications with cardiac or pulmonary arteriovenous shunts (e.g., cerebral emboli), and possibly multiinfarct dementia. The potential pathogenic role of SDs in these conditions is still to be clarified.

The data suggest that SD occurrence in the early phase of ischemia (i.e., within an hour after ischemia induction) is not tightly associated with immediate infarct evolution and maturation in this ischemic condition. However, a delayed onset of SD-related injury remains a potential risk.

Analysis of the hemodynamic responses with SDs indicated that similar hyperemic responses to SDs are coupled with various kinetics of Hb saturation during ischemia. Therefore, the SD-related CBF responses alone may have low predictive value as to the metabolic crisis during SD propagation in the tissue. Finally, the findings draw attention to the heterogeneity of hemodynamic correlates of ischemic SDs, which may determine the potential of SDs to cause injury.

DISCLOSURE/CONFLICT OF INTEREST

The authors declare no conflict of interest.

REFERENCES

1 Leão AAP. Spreading depression of activity in the cerebral cortex. *J Neurophysiol* 1944; **7**: 359–390.
2 Strong AJ, Fabricius M, Boutelle MG, Hibbins SJ, Hopwood SE, Jones R *et al.* Spreading and synchronous depressions of cortical activity in acutely injured human brain. *Stroke* 2002; **33**: 2738–2743.
3 Hartings JA, Watanabe T, Dreier JP, Major S, Vendelbo L, Fabricius M. Recovery of slow potentials in AC-coupled electrocorticography: application to spreading depolarizations in rat and human cerebral cortex. *J Neurophysiol* 2009; **102**: 2563–2575.
4 Somjen GG. Mechanisms of spreading depression and hypoxic spreading depression-like depolarization. *Physiol Rev* 2001; **81**: 1065–1096.
5 Hansen AJ, Quistorff B, Gjedde A. Relationship between local changes in cortical blood flow and extracellular K+ during spreading depression. *Acta Physiol Scand* 1980; **109**: 1–6.
6 Dreier JP, Körner K, Ebert N, Görner A, Rubin I, Back T *et al.* Nitric oxide scavenging by hemoglobin or nitric oxide synthase inhibition by N-nitro-L-arginine induces cortical spreading ischemia when K+ is increased in the subarachnoid space. *J Cereb Blood Flow Metab* 1998; **18**: 978–990.
7 Shin HK, Dunn AK, Jones PB, Boas DA, Moskowitz MA, Ayata C. Vasoconstrictive neurovascular coupling during focal ischemic depolarizations. *J Cereb Blood Flow Metab* 2006; **26**: 1018–1030.
8 Nedergaard M, Hansen AJ. Spreading depression is not associated with neuronal injury in the normal brain. *Brain Res* 1988; **449**: 395–398.
9 Dreier JP. The role of spreading depression, spreading depolarization and spreading ischemia in neurological disease. *Nat Med* 2011; **17**: 439–447.
10 Dreier JP, Woitzik J, Fabricius M, Bhatia R, Major S, Drenckhahn C *et al.* Delayed ischaemic neurological deficits after subarachnoid haemorrhage are associated with clusters of spreading depolarizations. *Brain* 2006; **129**(Pt 12): 3224–3237.
11 Mies G, Iijima T, Hossmann KA. Correlation between peri-infarct DC shifts and ischaemic neuronal damage in rat. *Neuroreport* 1993; **4**: 709–711.
12 Dijkhuizen RM, Beekwilder JP, van der Worp HB, Berkelbach van der Sprenkel JW, Tulleken KA, Nicolay K. Correlation between tissue depolarizations and damage in focal ischemic rat brain. *Brain Res* 1999; **840**: 194–205.
13 Dreier JP, Major S, Manning A, Woitzik J, Drenckhahn C, Steinbrink J *et al.* Cortical spreading ischaemia is a novel process involved in ischaemic damage in patients with aneurysmal subarachnoid haemorrhage. *Brain* 2009; **132**(Pt 7): 1866–1881.
14 Farkas E, Bari F, Obrenovitch TP. Multi-modal imaging of anoxic depolarization and hemodynamic changes induced by cardiac arrest in the rat cerebral cortex. *Neuroimage* 2010; **51**: 734–742.
15 Bere Z, Obrenovitch TP, Bari F, Farkas E. Ischemia-induced depolarizations and associated hemodynamic responses in incomplete global forebrain ischemia in rats. *Neuroscience* 2014; **260**: 217–226.
16 Traystman RJ. Animal models of focal and global cerebral ischemia. *ILAR J* 2003; **44**: 85–95.
17 Hossmann KA. Periinfarct depolarizations. *Cerebrovasc Brain Metab Rev* 1996; **8**: 195–208.
18 Miyake K, Takeo S, Kaijihara H. Sustained decrease in brain regional blood flow after microsphere embolism in rats. *Stroke* 1993; **24**: 415–420.
19 Mayzel-Oreg O, Omae T, Kazemi M, Li F, Fisher M, Cohen Y *et al.* Microsphere-induced embolic stroke: an MRI study. *Magn Reson Med* 2004; **51**: 1232–1238.
20 Nozari A, Dilekoz E, Sukhotinsky I, Stein T, Eikermann-Haerter K, Liu C *et al.* Microemboli may link spreading depression, migraine aura, and patent foramen ovale. *Ann Neurol* 2010; **67**: 221–229.

© 2014 ISCBFM

21 Clark D, Institoris Á, Kozák G, Bere Z, Tuor U, Farkas E *et al.* Impact of aging on spreading depolarizations induced by focal brain ischemia in rats. *Neurobiol Aging* 2014; doi:10.1016/j.neurobiolaging.2014.06.013 (in press).
22 Farkas E, Pratt R, Sengpiel F, Obrenovitch TP. Direct, live imaging of cortical spreading depression and anoxic depolarisation using a fluorescent, voltage-sensitive dye. *J Cereb Blood Flow Metab* 2008; **28**: 251–262.
23 Chen S, Li P, Luo W, Gong H, Zeng S, Luo Q. Origin sites of spontaneous cortical spreading depression migrated during focal cerebral ischemia in rats. *Neurosci Lett* 2006; **403**: 266–270.
24 Nakamura H, Strong AJ, Dohmen C, Sakowitz OW, Vollmar S, Sué M *et al.* Spreading depolarizations cycle around and enlarge focal ischaemic brain lesions. *Brain* 2010; **133**(Pt 7): 1994–2006.
25 Sonn J, Mayevsky A. Responses to cortical spreading depression under oxygen deficiency. *Open Neurol J* 2012; **6**: 6–17.
26 Zandt BJ, ten Haken B, van Putten MJ. Diffusing substances during spreading depolarization: analytical expressions for propagation speed, triggering, and concentration time courses. *J Neurosci* 2013; **33**: 5915–5923.
27 Aitken PG, Tombaugh GC, Turner DA, Somjen GG. Similar propagation of SD and hypoxic SD-like depolarization in rat hippocampus recorded optically and electrically. *J Neurophysiol* 1998; **80**: 1514–1521.
28 Röther J, de Crespigny AJ, D'Arceuil H, Mosley ME. MR detection of cortical spreading depression immediately after focal ischemia in the rat. *J Cereb Blood Flow Metab* 1996; **16**: 214–220.
29 Dreier JP, Kleeberg J, Petzold G, Priller J, Windmüller O, Orzechowski HD *et al.* Endothelin-1 potently induces Leão's cortical spreading depression in vivo in the rat: a model for an endothelial trigger of migrainous aura? *Brain* 2002; **125**(Pt 1): 102–112.
30 Martins-Ferreira H, Nedergaard M, Nicholson C. Perspectives on spreading depression. *Brain Res Brain Res Rev* 2000; **32**: 215–234.
31 Woitzik J, Hecht N, Pinczolits A, Sandow N, Major S, Winkler MK *et al.* Propagation of cortical spreading depolarization in the human cortex after malignant stroke. *Neurology* 2013; **80**: 1095–1102.
32 Fernandes de Lima VM, Hanke W. Modulation of CNS excitability by water movement. The D_2O effects on the non-linear neuron-glial dynamics. *J Biophys Chem* 2011; **2**: 353–360.
33 Koroleva VI, Bures J. Circulation of cortical spreading depression around electrically stimulated areas and epileptic foci in the neocortex of rats. *Brain Res* 1979; **173**: 209–215.
34 Hartings JA, Williams AJ, Tortella FC. Occurrence of nonconvulsive seizures, periodic epileptiform discharges, and intermittent rhythmic delta activity in rat focal ischemia. *Exp Neurol* 2003; **179**: 139–149.
35 Tsai MJ, Tsai YH, Kuo YM. Characterization of the pattern of ischemic stroke induced by artificial particle embolization in the rat brain. *Biomaterials* 2011; **32**: 6381–6388.
36 Ayata C. Spreading depression and neurovascular coupling. *Stroke* 2013; **44**(6 Suppl 1): S87–S89.
37 Sun X, Wang Y, Chen S, Luo W, Li P, Luo Q. Simultaneous monitoring of intracellular pH changes and hemodynamic response during cortical spreading depression by fluorescence-corrected multimodal optical imaging. *Neuroimage* 2011; **57**: 873–884.
38 Dunn AK, Devor A, Bolay H, Andermann ML, Moskowitz MA, Dale AM *et al.* Simultaneous imaging of total cerebral hemoglobin concentration, oxygenation, and blood flow during functional activation. *Opt Lett* 2003; **28**: 28–30.
39 Wolf T, Lindauer U, Reuter U, Back T, Villringer A, Einhäupl K *et al.* Noninvasive near infrared spectroscopy monitoring of regional cerebral blood oxygenation changes during peri-infarct depolarizations in focal cerebral ischemia in the rat. *J Cereb Blood Flow Metab* 1997; **17**: 950–954.

© 2014 ISCBFM